Factors That Drive Peptide Assembly and Fibril Formation: Experimental and Theoretical Analysis of Sup35 NNQQNY Mutants

Thanh D. Do,[±] *Nicholas J. Economou,*[±] *Nichole E. LaPointe,*[†] *William M. Kincannon,*[±] *Christian Bleiholder,*[±] *Stuart C. Feinstein,*[†] *David B. Teplow,*[&] *Steven K. Buratto,*[±] *and Michael T. Bowers*[±,*]

[±]Department of Chemistry and Biochemistry, University of California, Santa Barbara, California, 93106, U.S.A.

[†]Neuroscience Research Institute and Department of Molecular, Cellular and Developmental Biology, University of California, Santa Barbara, California, 93106, U.S.A.

[&]Department of Neurology, David Geffen School of Medicine at UCLA, Mary S. Easton Center for Alzheimer's Disease Research at UCLA, and Brain Research Institute and Molecular Biology Institute, University of California, Los Angeles, California 90095, U.S.A.

*Correspondence to: bowers@chem.ucsb.edu

SUPPLEMENTARY INFORMATION

1. Rosetta C-scores from ZipperDB

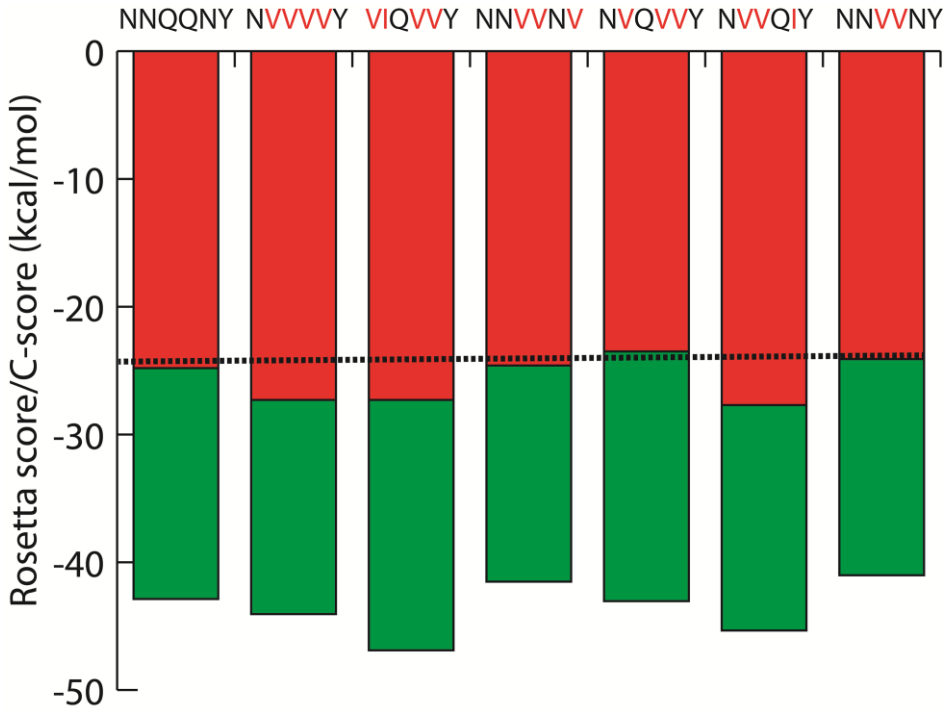

Figure S1. Fibrillar propensity profiles of NNQQNY and its mutants. Each histogram bar represents the Rosetta score (red) and C-score (green) of one hexapeptide. The peptides whose Rosetta scores are below the threshold of -23 kcal/mol are predicted to form fibrils, shown by the dashed line above.

S2.TEM

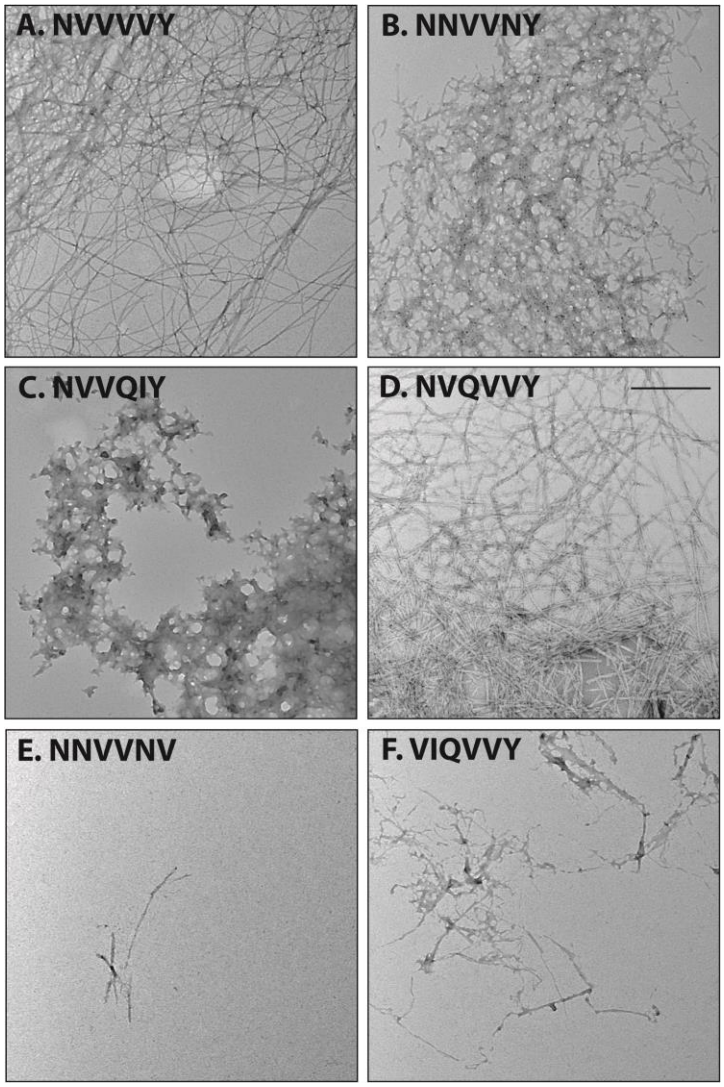

Figure S2. Representative TEM images of aggregates of the six peptides. **A.** NVVVVY shows abundant long, fibrillar aggregates. **B.** NNVVNY forms abundant short fibrillar aggregates. **C.** NVVQIY forms some fibers and some densely packed non fibrillar aggregates. **D.** NVQVVY forms abundant, fibrillar aggregates. **E.** NNVVNV shows either no aggregates or very few, poorly defined fibers. **F.** VIQVVY forms few, poorly defined fibers. The scale bar is 500 nm.

S3. Explicit solvent molecular dynamics

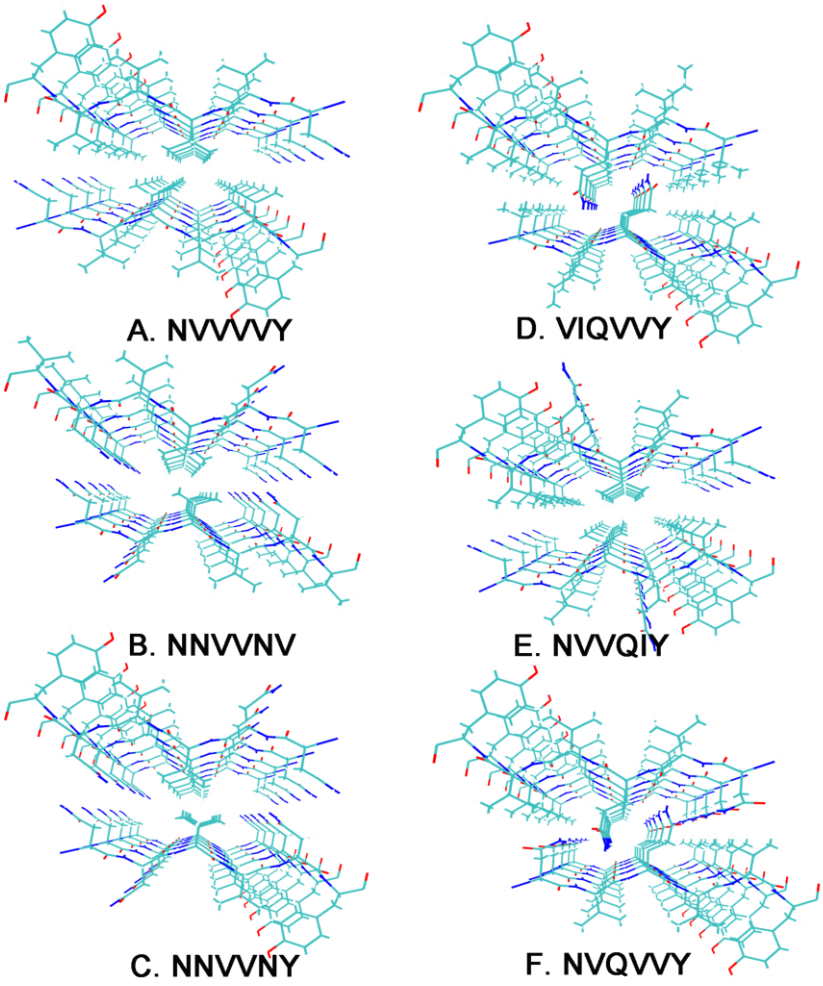

Figure S3. Steric zipper starting conformations for molecular dynamics simulations of peptide decamers. **A**. NVVVVY, **B**. NNVVNV, **C**. NNVVNY, **D**. VIQVVY, **E**. NVVQIY and **F**. NVQVVY.

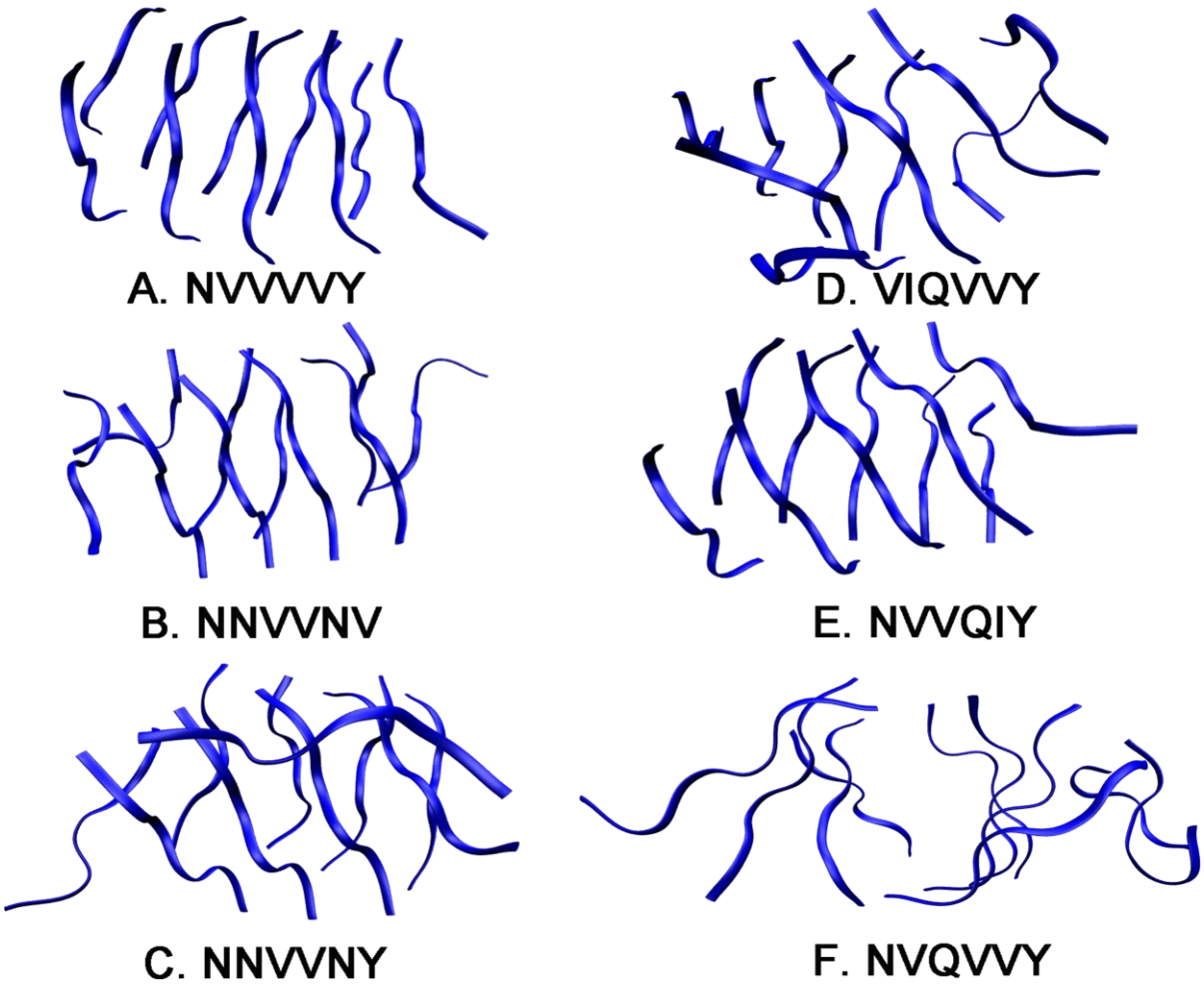

Figure S4. Final conformations obtained from molecular dynamics simulations starting with steric zipper peptide decamers . **A**. NVVVVY, **B**. NNVVNV, **C**. NNVVNY, **D**. VIQVVY, **E**. NVVQIY and **F**. NVQVVY.

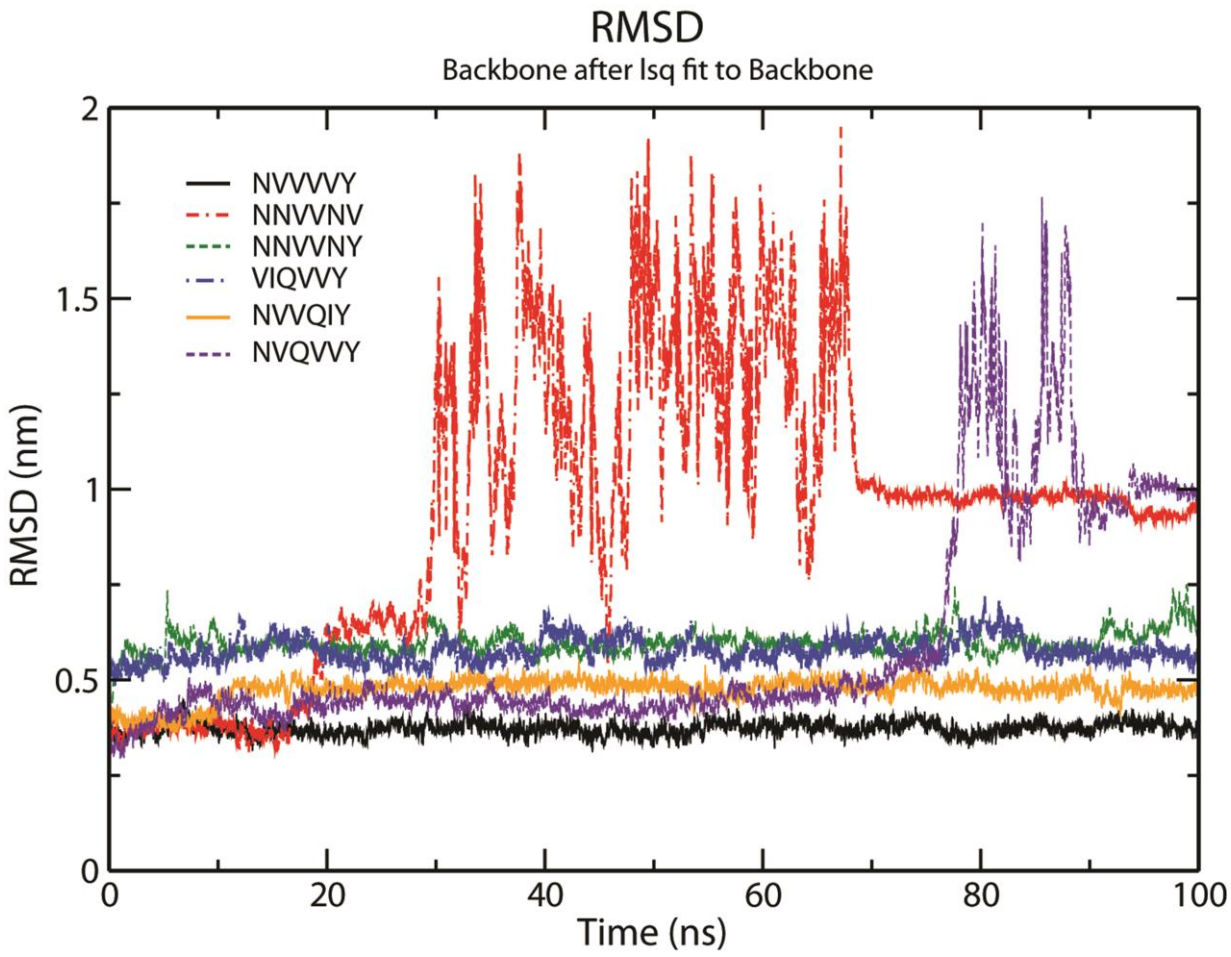

Figure S5. Backbone RMSD computed for 100-ns molecular dyanimic simulations starting with steric zipper decamers. Structures with average RMSD fluctuations less than 0.5 nm are considered as stable (NVVVVY and NVVQIY). NVQVVY and NNVVNY are relatively stable. VIQVVY is in the borderline. NNVVNV decamer is not stable.

S4.1. Ion mobility mass spectrometry[1]

In IM-MS, the ions are generated by electrosprayed ionization and stored in an ion funnel. The ions are either passed to a mass detector to obtained a mass spectrum, or subsequently pulsed into a drift cell filled with He at high pressure (12-13 torr). The ions experience the influence of a weak electrical field and collision with He buffer gas. The forces cancel each other and as a result, the ions travel with a constant velocity. At the end of the drift tube the ions are collected by a second ion funnel where they are steered and focused into a quadrupole mass filter for mass selection and subsequently are detected as a function of time in the arrival time distribution (ATD). Experimental collision cross section in He gas are measured by mass-selecting peaks in the mass spectrum by their *m/z* value, and recording ATDs at different drift voltages *V* (with *V* ~ 1800, 2300, 2800 and 3300) for each selected *m/z* value. The center of each peak in a particular ATD is taken as arrival time t_a and plotted as a function of the *p/V* ratio (where *V* is the drift voltage; see Eq. 1.3). The slope of this correlation is related to the mobility K_0 of the corresponding feature, which in turn is inversely proportional to the collision cross-section. All factors in these equations are either universal constants or parameters that were accurately measured in the experiment. The collision cross-sections are determined with an accuracy of ±1%. This instrument is denoted as the high-pressure instrument.

Ions that are injected into the drift cell experience a constant force from the electric field, *E*, which is balanced by a retarding frictional force due to collisions with the buffer gas. Under these conditions the velocity, υ_d, at which the ions move through the buffer gas is proportional to the magnitude of the electric field where the mobility, *K* is the proportionality constant:

(1.1) $$\vec{\upsilon}_d = K\vec{E}$$

The absolute mobility of the ion packet is dependent on the temperature and the pressure of the buffer gas so it is customary to use the reduced mobility K_0.

(1.2) $$K_0 = \left(K \cdot \frac{p}{760\text{torr}} \cdot \frac{273.16\text{K}}{T} \right)$$

After the ions exit the drift cell they are mass analyzed and detected as a function of the arrival time, t_A. The reduced mobility can be determined from instrumental parameters by converting equation (1.1) to equation (1.3) and plotting t_A versus *p/V*.[2]

(1.3) $$t_A = \frac{l^2}{K_0} \cdot \frac{273.16\text{K}}{760\text{torr} \cdot T} \cdot \frac{p}{V} + t_0$$

In equation 1.3, *l* is the length of the drift cell, *p* is the gas pressure in torr, *V* is the voltage across the cell, and t_0 is the time the ions spend outside the drift cell before hitting the detector.

Collision theory relates K_0 to σ, the collision cross section of the ion of interest:[3]

(1.4) $$K_0 = \frac{3q}{16N} \left(\frac{2\pi}{\mu k_b T} \right)^{1/2} \frac{1}{\sigma}$$

Here, *N* is the buffer gas number density, μ is the reduced mass of the collision system (ion + He) and k_b is Boltzmann's constant. The collision cross sections are reported as the average of multiple

measurements, typically more than three, and all measurements are reproducible within 1%. All data presented in the manuscript and SI is given as raw data, with no smoothing and no post-processing.

The measured reduced mobility (K_0) and subsequently the collision cross section (σ) contain information about the three dimensional configuration of the ion.

The flux of ions exiting the drift tube can be calculated[3] and is used to fit the experimental arrival time distributions. It is assumed that the ion packet takes the form of a periodic delta function and the flux is given by equation 1.5.

(1.5)
$$\Phi(0,z,t) = \frac{s \cdot a \cdot e^{-\alpha \cdot t}}{4(\pi D_L t)^{1/2}} \cdot \left(v_d + \frac{z}{t}\right) \cdot \left[1 - e^{\left(-r_0^2 / 4D_T t\right)}\right] \cdot e^{\left(-(z - v_d \cdot t)^2 / 4D_L t\right)}$$

Here z is the distance travelled by the ions, r_0 is the radius of the initial ion packet, a is the area of the exit aperture, D_L and D_T are the longitudinal and transverse diffusion coefficients, s is the initial ion density and α is the loss of ions due to reactions in the drift tube.

S4.2. Representative ATDs

Representative arrival time distributions (ATDs) for peaks with *m/z* values indicated in the mass spectra of the peptides (Fig.2 in the main text). The ATDs were obtained at the drift voltage of ~3330V and pressue of 12.5-13.5 torr. Each feature is labeled by oligomer size to charge ratios (*n/z*) and its cross section in squared angstroms.

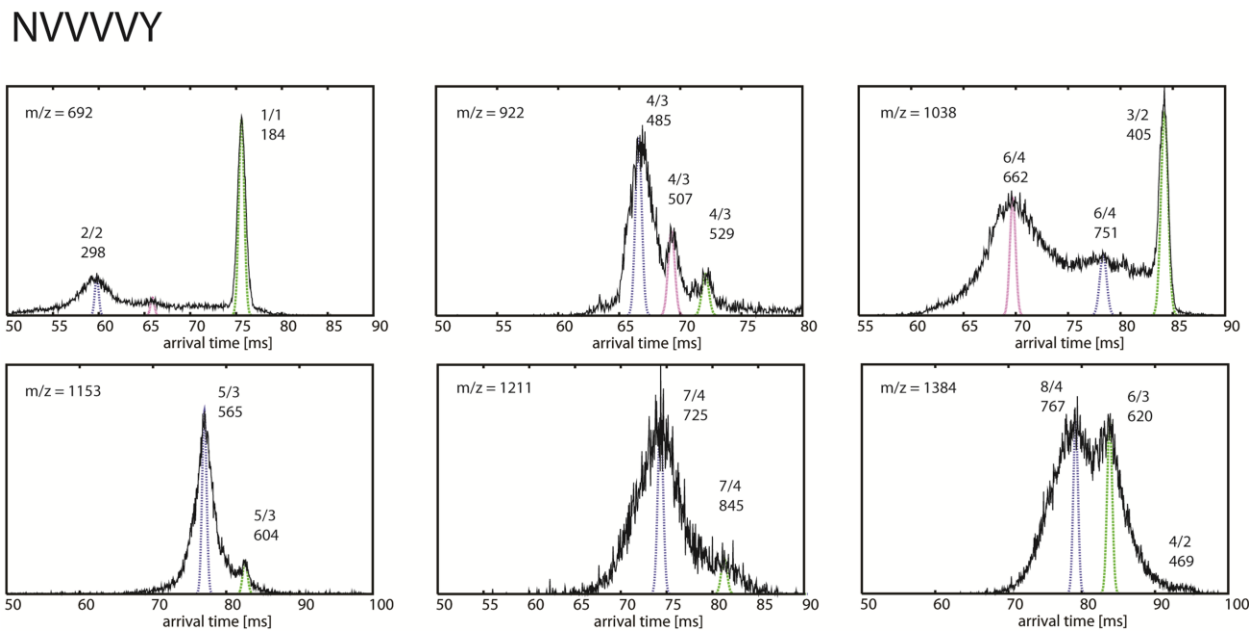

Figure S6. Representative ATDs of NVVVVY. The narrow colored peaks are predictions of Equation 1.5 for a single conformer.

NNVVNY

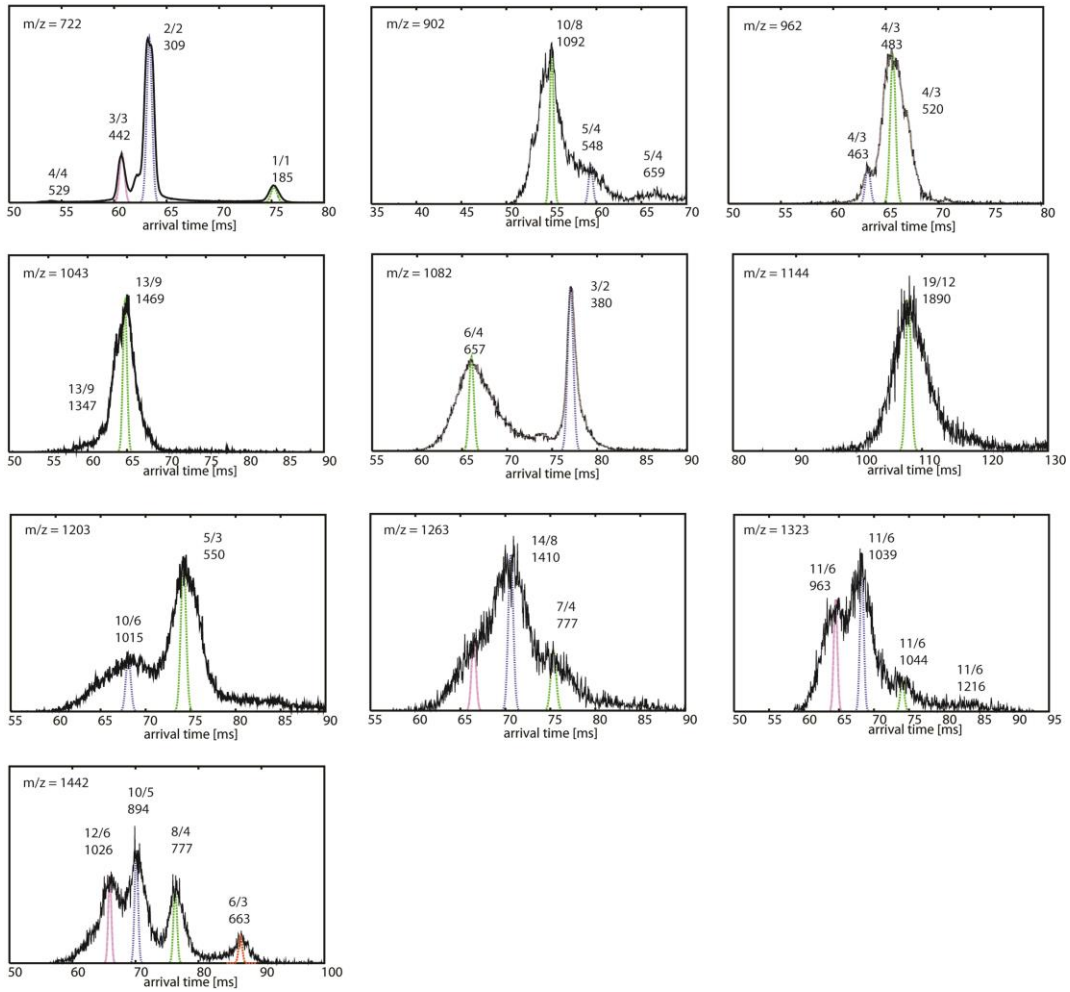

Figure S7. Representative ATDs of NNVVNY. The narrow colored peaks are predictions of Equation 1.5 for a single conformer.

NVVQIY

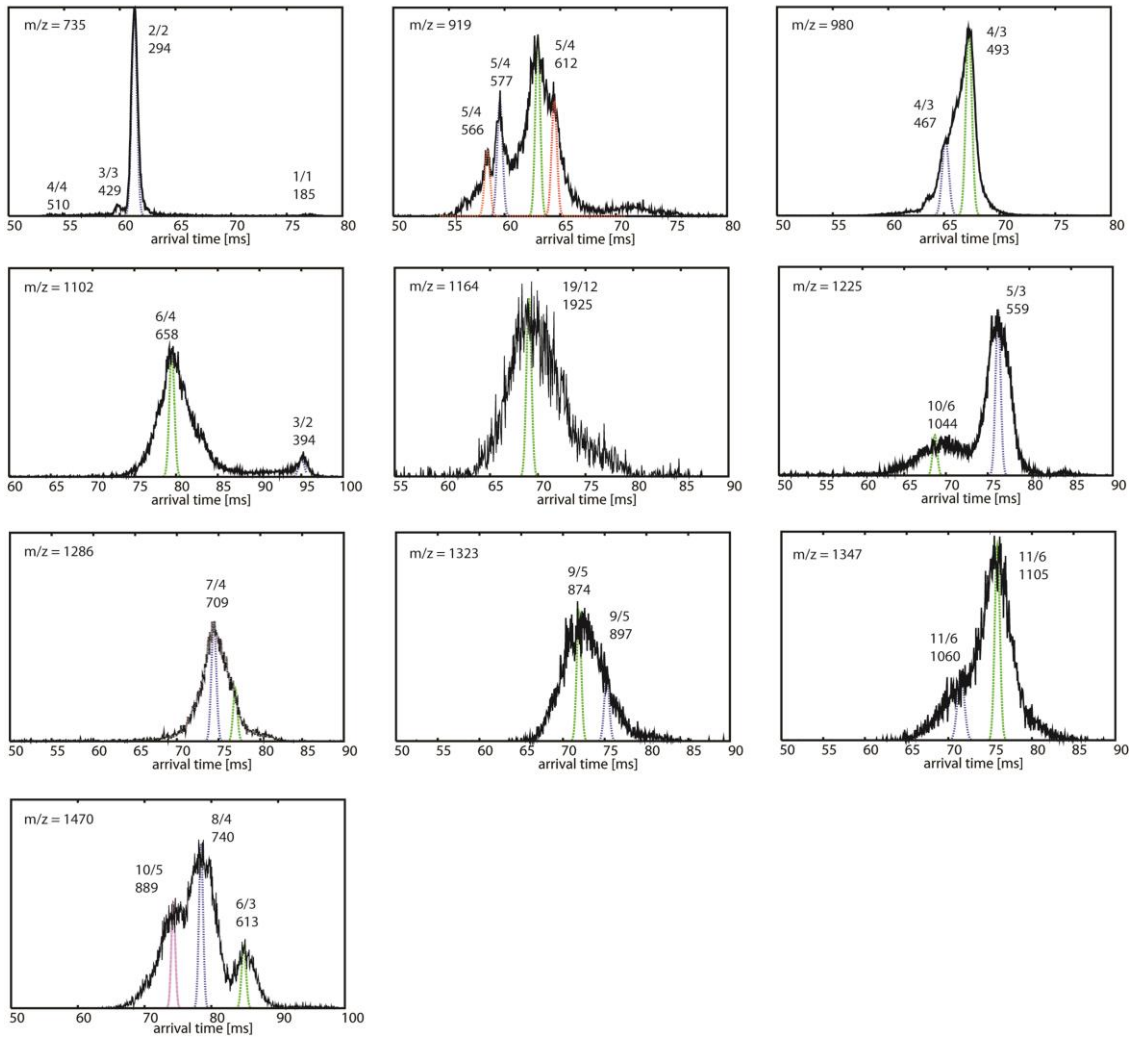

Figure S8. Representative ATDs of NVVQIY. The narrow colored peaks are predictions of Equation 1.5 for a single conformer.

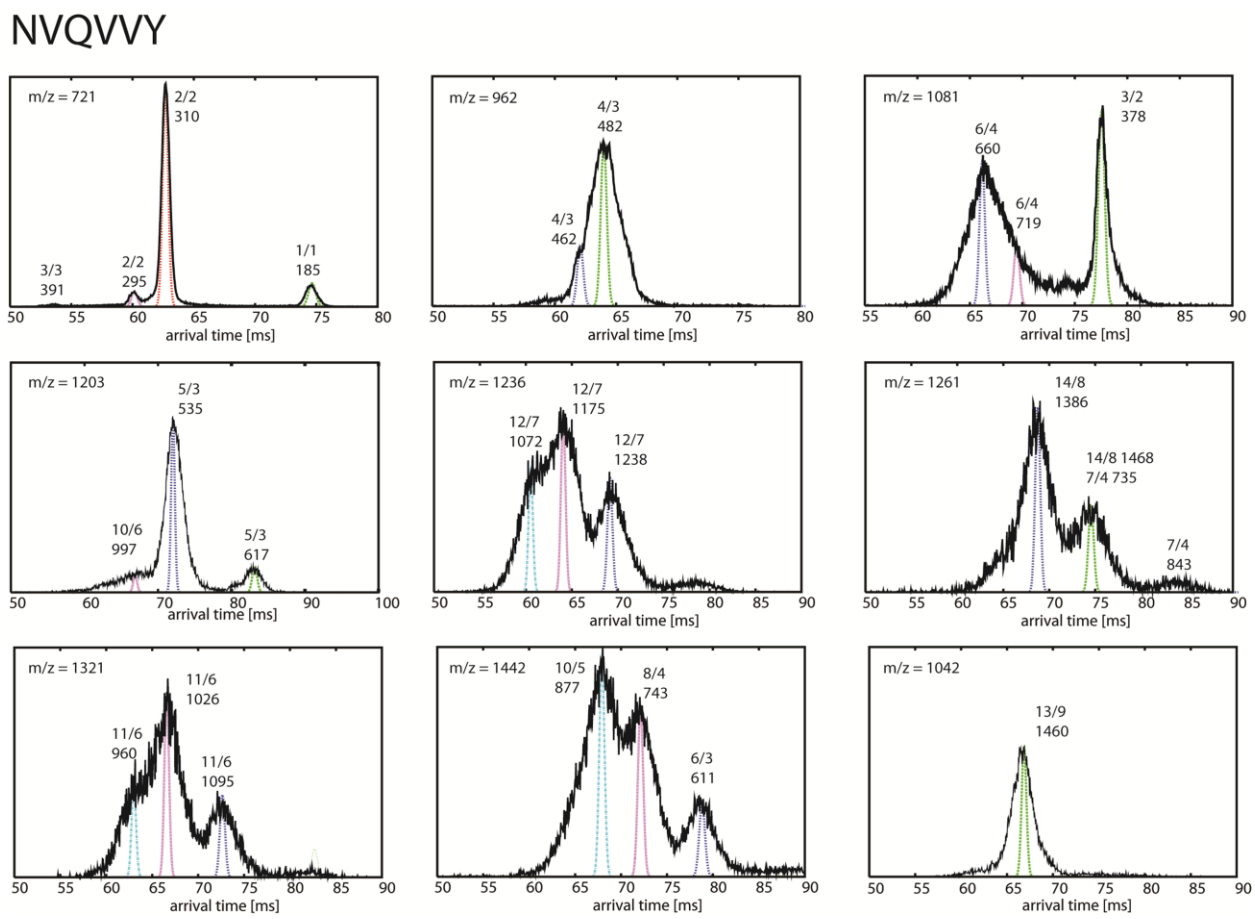

Figure S9. Representative ATDs of NVQVVY. The narrow colored peaks are predictions of Equation 1.5 for a single conformer.

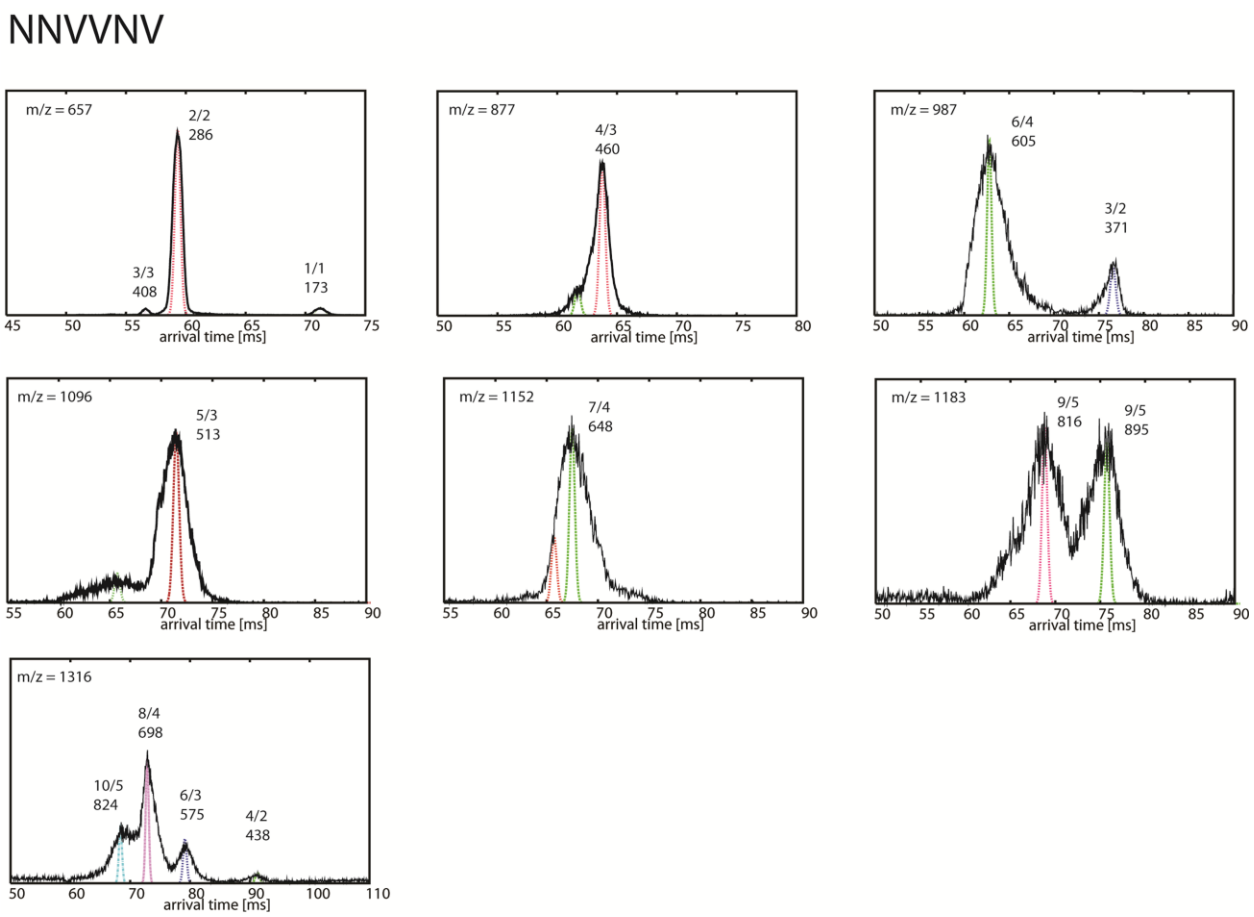

Figure S10. Representative ATDs of NNVVNV. The narrow colored peaks are predictions of Equation 1.5 for a single conformer.

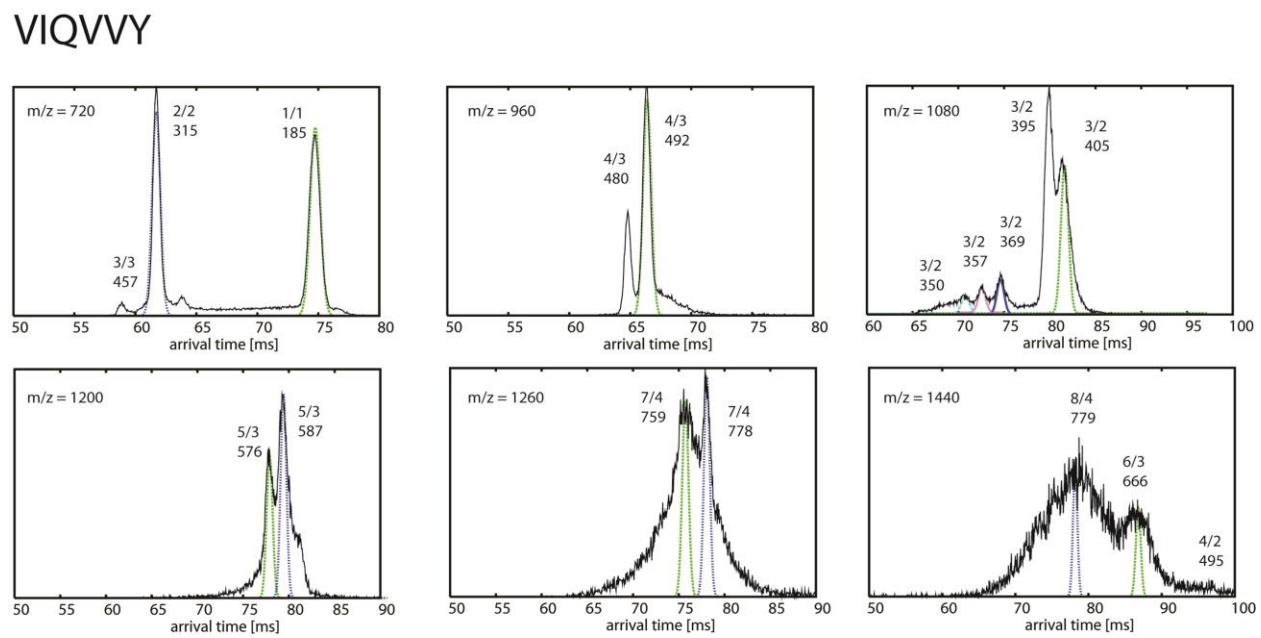

Figure S11. Representative ATDs of VIQVVY. The narrow colored peaks are predictions of Equation 1.5 for a single conformer.

1. Wyttenbach, T.; Bowers, M. T., Gas-phase conformations: The ion mobility/ion chromatography method. *Modern Mass Spectrometry* **2003,** *225*, 207-232.
2. Gidden, J.; Baker, E. S.; Ferzoco, A.; Bowers, M. T., Structural Motifs of DNA Complexes in the Gas Phase. *Int. J. Mass Spectrom. Ion Proc.* **2005,** *240*, 183-193.
3. Mason, E. A.; McDaniel, E. W., *Transport Properties of Ions in Gases*. Wiley: 1988.